From monomeric to polymeric manganese complexes bearing bis(imino)pyridine and related ligands

Vernon C. Gibson,* Stuart McTavish, Carl Redshaw, Gregory A. Solan, Andrew J. P. White and David J. Williams

Department of Chemistry, Imperial College, South Kensington, London, UK SW7 2AY.
E-mail: V.Gibson@ic.ac.uk

Reactions of MnX_2 with the tridentate nitrogen donor ligands [2,6-{(2,4,6-Me$_3$C$_6$H$_2$)N=CMe}$_2$C$_5$H$_3$N], [2,6-{(Me)-(Ph)NN=CMe}$_2$C$_5$H$_3$N] and [2-{(2,6-Pr$^i_2$C$_6$H$_3$)N=CH}-6-{(2,6-Pr$^i_2$C$_6$H$_3$)NHCH(Me)}C$_5$H$_3$N] in refluxing acetonitrile yield the high spin divalent monometallic manganese complexes, [2,6-{(2,4,6-Me$_3$C$_6$H$_2$)N=CMe}$_2$C$_5$H$_3$N]-MnX$_2$ (X = Br **1**), [2,6-{(Me)(Ph)NN=CMe}$_2$C$_5$H$_3$N]MnX$_2$ (X = Cl **2**) and [2-{(2,6-Pr$^i_2$-C$_6$H$_3$)N=CH}-6-{(2,6-Pr$^i_2$-C$_6$H$_3$)NHCH(Me)}C$_5$H$_3$N]MnX$_2$ (X = Cl **3**), respectively, in good yield. Crystallographic studies on **1**–**3** reveal all three complexes to be pentacoordinate with geometries that can be best described as distorted trigonal bipyramidal (**1**, **2**) or square pyramidal (**3**). Conversely, treatment of $MnCl_2$ with [2-{(2″-H$_2$NC$_6$H$_4$–C$_2$H$_4$–2″-C$_6$H$_4$)N=CMe}-6-{O=CMe}C$_5$H$_3$N] (prepared from the incomplete condensation reaction of the diamine [{2,2″-(NH$_2$)C$_6$H$_4$}$_2$-(CH$_2$CH$_2$)] with 2,6-diacetylpyridine) under similar reaction conditions results in self-assembly to afford the antiferromagnetically coupled polymetallic salt [{2,6-{(2′,2″-C$_6$H$_4$–CH$_2$)$_2$(N=CMe)$_2$}$_2$(C$_5$H$_3$N)$_2$}Mn$_2$Cl$_3$(NCMe)$_2$]-[{2,6-{(2′,2″-C$_6$H$_4$–CH$_2$)$_2$(N=CMe)$_2$}$_2$(C$_5$H$_3$N)$_2$}Mn$_2$Cl$_3$(MnCl$_4$)]$_n$ (**4**). The molecular structure of **4** shows a discrete dimanganese cation and polymeric manganese anion with each ionic unit supported by a 26-membered macrocyclic hexadentate nitrogen donor ligand.

Introduction

In recent years there has been much interest in the discovery and development of new catalysts for olefin polymerisation. While cyclopentadienyl-based systems have largely led the way,[1] the potential for non-cyclopentadienyl metal catalysts, and especially for new systems featuring late transition metals, has been realised.[2–4] In this regard, divalent iron (d^6) and cobalt (d^7) complexes stabilised by sterically demanding bis(imino)pyridine ligands (type **A** in Fig. 1) have allowed access to highly active
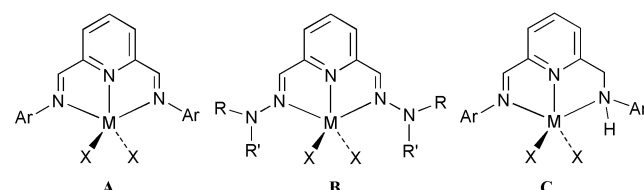

Fig. 1 Bis(imino)pyridine (**A**), bis(hydrazone)pyridine (**B**) and aminoiminopyridine (**C**) complexes.

catalysts for ethylene polymerisation.[5,6] Subsequent advances have shown that active systems can also be prepared containing the bis(hydrazone)pyridine (type **B** in Fig. 1)[7] and the aminoiminopyridine (type **C** in Fig. 1)[8] complexes, albeit with lower productivities.

By contrast, manganese (d^5) derivatives of complexes **A**–**C** (Fig. 1) exhibit no or very poor ethylene polymerisation activities upon activation with excess methylaluminoxane (MAO), possibly a result of reduction of the Mn(II) centres.[5c,9] The recent report by Gambarotta and co-workers[9] on the bis(imino)-pyridine manganese system prompts us to disclose our results on the synthesis and characterisation of Mn(II) complexes containing bis(imino)pyridine, and closely related bis(hydrazone)-pyridine and aminoiminopyridine, ligands.

Results and discussion

Synthesis of ligands and complexes

The bis(imino)pyridine, bis(hydrazone)pyridine and the amino-iminopyridine manganese complexes [2,6-{(2,4,6-Me$_3$C$_6$H$_2$)N=CMe}$_2$C$_5$H$_3$N]MnBr$_2$ (**1**), [2,6-{(Me)(Ph)NN=CMe}$_2$C$_5$H$_3$N]-MnCl$_2$ (**2**) and [2-{(2,6-Pr$^i_2$C$_6$H$_3$)N=CH}-6-{(2,6-Pr$^i_2$C$_6$H$_3$)N-HCH(Me)}C$_5$H$_3$N]MnCl$_2$ (**3**) have been prepared in good yield (*ca.* 40–77%) as air stable orange solids by reaction of the corresponding ligand with MnX_2 in refluxing acetonitrile (Scheme 1). All the complexes have been characterised by mass spectrometry, infrared spectroscopy, EPR, microanalysis and from magnetic measurements (see Experimental). In addition, **1**–**3** have been the subject of single crystal X-ray diffraction studies.

Orange crystals of **1** suitable for an X-ray crystal structure determination were grown from acetonitrile at room temperature. The molecular structure is shown in Fig. 2; selected bond
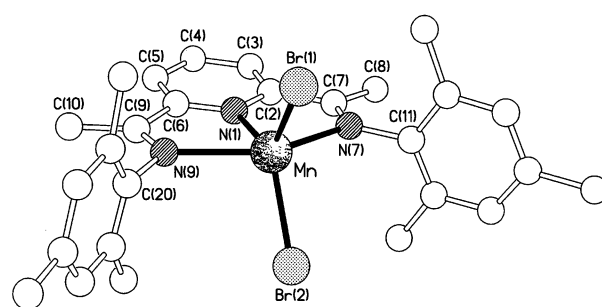

Fig. 2 The molecular structure of **1**.

lengths and angles are listed in Table 1. The manganese complex **1** crystallises with two independent molecules in the asymmetric unit, both having molecular C_s symmetry and a trigonal bipyramidal geometry for the manganese centre. This geometry is similar to that observed for the related complex [2,6-{(C$_6$H$_5$)N=CMe}$_2$C$_5$H$_3$N]MnBr$_2$.[10] The Mn–N and Mn–Br distances are unexceptional (Table 1). The principal difference between the two molecules is in the displacement of the metal centre out of the plane of the bis(imino)pyridine unit. In one molecule the manganese lies only 0.08 Å out of the plane of the ligand backbone, which is planar to within 0.04 Å, whereas in the other the metal is displaced by 0.24 Å out of the ligand plane (which is planar to within 0.06 Å). In the isostructural

Table 1 Selected bond lengths (Å) and angles (°) for **1**

	Molecule A	Molecule B		Molecule A	Molecule B
Mn–Br(1)	2.497(2)	2.498(2)	Mn–Br(2)	2.485(2)	2.483(2)
Mn–N(1)	2.202(7)	2.207(6)	Mn–N(7)	2.330(7)	2.322(6)
Mn–N(9)	2.330(6)	2.345(6)	C(7)–N(7)	1.270(10)	1.272(10)
C(9)–N(9)	1.292(10)	1.277(10)			
N(1)–Mn–N(9)	71.2(2)	71.2(2)	N(1)–Mn–N(7)	71.3(2)	70.6(2)
N(9)–Mn–N(7)	142.6(2)	141.3(2)	N(1)–Mn–Br(2)	125.3(2)	130.6(2)
N(9)–Mn–Br(2)	99.3(2)	101.0(2)	N(7)–Mn–Br(2)	100.9(2)	99.3(2)
N(1)–Mn–Br(1)	122.2(2)	117.6(2)	N(9)–Mn–Br(1)	100.2(2)	99.5(2)
N(7)–Mn–Br(1)	100.8(2)	103.0(2)	Br(2)–Mn–Br(1)	112.51(6)	111.79(6)
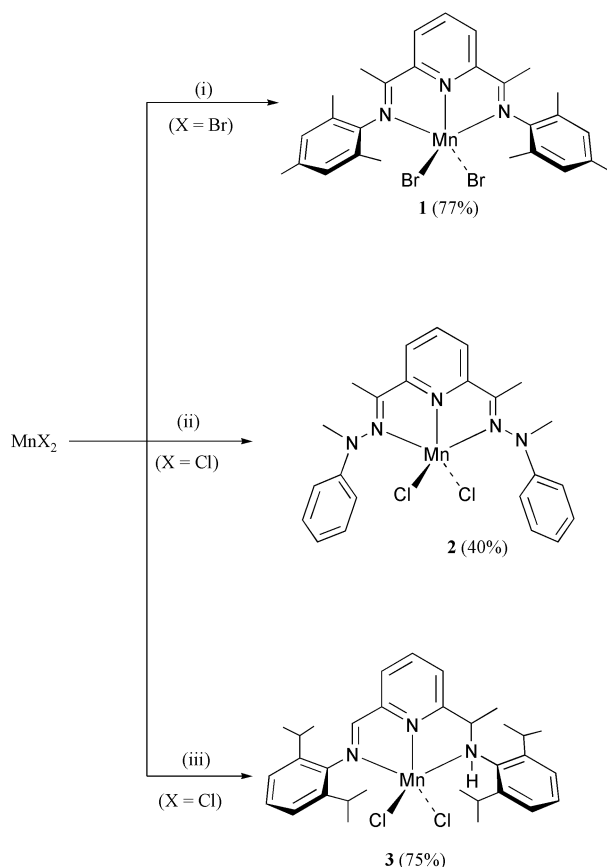
Scheme 1 Reagents and conditions: (i) [2,6-{(2,4,6-Me$_3$C$_6$H$_2$)N=CMe}$_2$C$_5$H$_3$N], MeCN, heat; (ii) [2,6-{(Me)(Ph)NN=CMe}$_2$C$_5$H$_3$N], MeCN, heat; (iii) [2-{(2,6-Pr$^i_2$C$_6$H$_3$)N=CH}-6-{(2,6-Pr$^i_2$C$_6$H$_3$)NHCH-(Me)}C$_5$H$_3$N], MeCN, heat.

Table 2 Selected bond lengths (Å) and angles (°) for **2**

Mn–Cl(1)	2.353(2)	Mn–Cl(2)	2.332(2)
Mn–N(1)	2.173(4)	Mn–N(8)	2.330(4)
Mn–N(11)	2.321(4)	C(7)–N(8)	1.290(7)
N(8)–N(9)	1.396(6)	C(10)–N(11)	1.285(7)
N(11)–N(12)	1.387(6)		
N(1)–Mn–N(11)	71.9(2)	N(1)–Mn–N(8)	71.2(2)
N(11)–Mn–N(8)	143.0(2)	N(1)–Mn–Cl(2)	122.96(13)
N(11)–Mn–Cl(2)	99.65(12)	N(8)–Mn–Cl(2)	97.91(13)
N(1)–Mn–Cl(1)	109.25(12)	N(11)–Mn–Cl(1)	97.35(12)
N(8)–Mn–Cl(1)	97.18(12)	Cl(2)–Mn–Cl(1)	127.77(7)

Fig. 3 The molecular structure of **2**.
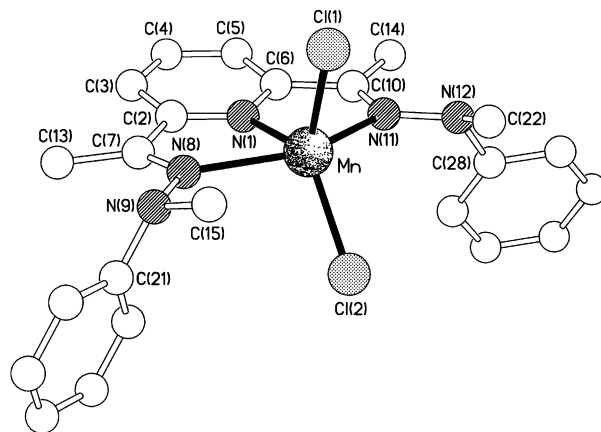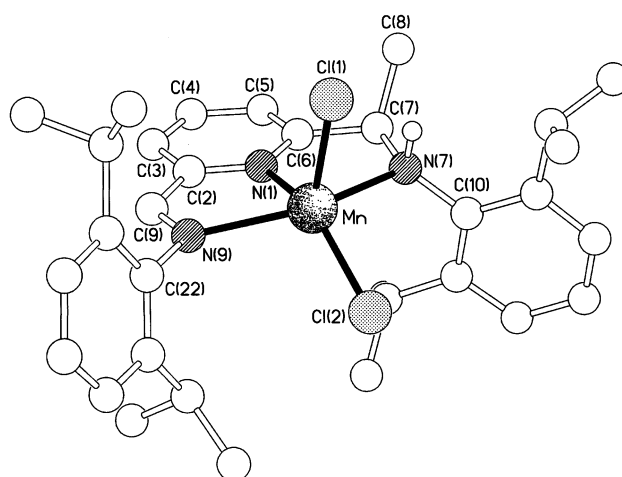

Fig. 4 The molecular structure of **3**.

(though not isomorphous) iron complex [5b] the metal lies 0.15 Å out of the ligand plane. In both independent molecules the mesityl ring planes are oriented approximately orthogonally to the plane of the bis(imino)pyridine unit (interplanar angles in the range 80–89°). There are no intermolecular packing features of interest.

The molecular structure of **2** is shown in Fig. 3; selected bond lengths and angles are listed in Table 2. Crystals of **2** were grown from acetonitrile at room temperature. Compound **2** has a solid state structure that is isomorphous with its iron analogue,[7] having molecular C_s symmetry and a distorted trigonal bipyramidal geometry at the manganese atom, though with the Mn–Cl(1) distance still being significantly longer than that to Cl(2); the Mn–N distances are unexceptional. The bis(imino)-pyridine unit, together with N(9) and N(12), is planar to within 0.08 Å, the manganese atom being displaced by 0.16 Å out of the plane in the direction of Cl(1). There are no intermolecular packing interactions of note.

The molecular structure of **3** is shown in Fig. 4; selected bond lengths and angles are collected in Table 3. A single crystal X-ray analysis shows the manganese complex **3** to be isomorphous with the previously reported iron and cobalt analogues.[8] The geometry at manganese is square pyramidal with the metal atom lying 0.53 Å out of the basal plane *cf.* 0.43 Å for the iron species. The aminoiminopyridine unit is planar to within 0.07 Å with the manganese centre lying 0.16 Å out of this plane in the direction of Cl(1). The planes of the

Table 3 Selected bond lengths (Å) and angles (°) for **3**

Mn–Cl(1)	2.327(2)	Mn–Cl(2)	2.2967(12)
Mn–N(1)	2.206(4)	Mn–N(7)	2.386(4)
Mn–N(9)	2.294(4)	C(7)–N(7)	1.480(6)
C(9)–N(9)	1.268(6)		
N(1)–Mn–N(9)	73.35(13)	N(1)–Mn–Cl(2)	144.11(12)
N(9)–Mn–Cl(2)	103.30(10)	N(1)–Mn–Cl(1)	103.98(12)
N(9)–Mn–Cl(1)	106.12(12)	Cl(2)–Mn–Cl(1)	111.05(7)
N(1)–Mn–N(7)	71.63(14)	N(9)–Mn–N(7)	144.16(14)
Cl(2)–Mn–N(7)	100.51(10)	Cl(1)–Mn–N(7)	89.58(12)

C(10)- and C(22)-containing 2,6-diisopropylphenyl rings are inclined by *ca.* 88 and 78° to the aminoiminopyridine unit respectively. The most noticeable feature of the pattern of bonding to manganese is the very long Mn–N distance to the amino nitrogen N(7) [2.386(4) Å] *cf.* that to the imino nitrogen N(9) [2.294(4) Å], a very similar asymmetry to that seen in the iron complex. There are no noteworthy intermolecular packing interactions.

Complexes **1**–**3** are all paramagnetic with magnetic moments falling between 5.6 and 5.8 μ_B (Evans balance at ambient temperature) indicating a high spin d^5 electronic configuration for the divalent manganese centres. The *X*-band EPR spectra of **1**–**3**, recorded at ambient temperature in toluene display single broad featureless resonances at *ca.* $g = 2.0$; no hyperfine structure is evident. The IR spectra of **1**–**3** display absorption bands for the imine C=N stretches *ca.* 1590 cm^{-1} and for **3** an additional band at 3270 cm^{-1} is observed for the ν(N–H). In the FAB mass spectra of **1**–**3** molecular ion peaks are seen along with peaks corresponding to loss of halide ligands from the molecular ions.

With the intent of generating complexes with the bis(imino)pyridine motif (type **A** in Fig. 1) incorporated into a macrocyclic unit, we set about examining the reaction of 2,6-diacetylpyridine with the *ortho*-bridged diamine [{2,2′-(NH$_2$)-C$_6$H$_4$}$_2$(CH$_2$CH$_2$)]. However, the acid catalysed condensation in ethanol at elevated temperature afforded [2-{(2′-H$_2$NC$_6$H$_4$–C$_2$H$_4$–2″-C$_6$H$_4$)N=CMe}-6-{O=CMe}C$_5$H$_3$N] as a yellow solid, in which only one amine group had undergone condensation and the other amine remained unreacted. Spectroscopic data (see Experimental) are consistent with the formulation depicted in Scheme 2. The ^{1}H NMR spectrum of [2-{2′-H$_2$NC$_6$H$_4$–C$_2$H$_4$–2″-C$_6$H$_4$N=CMe}-6-{O=CMe}C$_5$H$_3$N] in CDCl$_3$ exhibits resonances in the regions characteristic of the imine (δ 2.41) and ketone (δ 2.80) CMe protons along with three more downfield signals (δ 8.61–7.95) being observed for the inequivalent pyridine protons. In the infrared spectrum absorption bands for the imine and ketone are clearly visible at 1696 and 1638 cm^{-1} respectively and the molecular ion peak is observed in the EI mass spectrum.

Complete condensation can, nevertheless, be achieved on reaction of MnCl$_2$ with [2-{2′-H$_2$NC$_6$H$_4$–C$_2$H$_4$–2″-C$_6$H$_4$N=CMe}-6-{O=CMe}C$_5$H$_3$N] in refluxing acetonitrile to afford the air stable orange crystalline salt [LMn$_2$Cl$_3$(NCMe)$_2$]-[LMn$_2$Cl$_3$(MnCl$_4$)]$_n$ (**4**) [where L = 2,6-{(2′,2″-C$_6$H$_4$–CH$_2$)$_2$-(N=CMe)$_2$}$_2$(C$_5$H$_3$N)$_2$] (Scheme 2).

Single crystals of **4** suitable for an X-ray crystal determination were grown by slow cooling of a hot acetonitrile solution of **4**. The molecular structure indicates that co-crystallisation of two distinct molecular species has occurred. One of these is an anionic polymer in which macrocyclic LMn$_2$Cl$_3$ moieties (Fig. 5) are linked by MnCl$_4$ dianions to form chains having a continuous –Mn–Cl–Mn–Cl– backbone (Fig. 6). The other, in contrast, comprises discrete [LMn$_2$Cl$_3$(NCMe)$_2$] cations (Fig. 7).

In both cases the LMn$_2$Cl$_3$ cores have crystallographic C_2 symmetry and essentially the same geometry, the manganese, nitrogen and equivalent chlorine atoms fitting to within 0.16 Å. The geometry at each manganese of the LMn$_2$Cl$_3$ units is
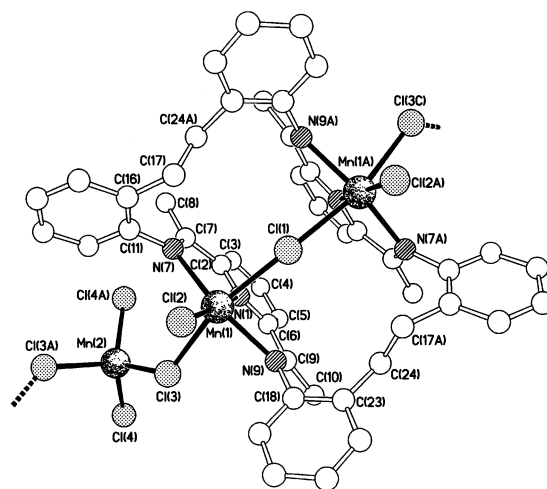
**Fig. 5** The structure of one of the repeat units of the anionic [{2,6-{(2′,2″-C$_6$H$_4$–CH$_2$)$_2$(N=CMe)$_2$}$_2$(C$_5$H$_3$N)}Mn$_2$Cl$_3$(MnCl$_4$)]$_n$ polymer chains present in the crystals of **4**.
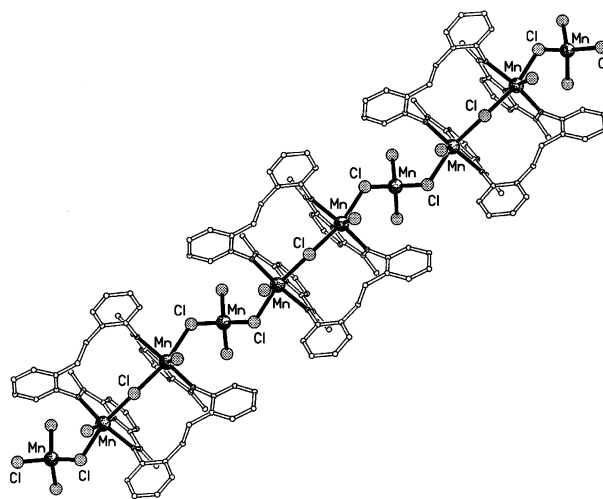
Fig. 6 Part of the one of the MnCl$_4$-linked anionic polymer chains of [{2,6-{(2′,2″-C$_6$H$_4$–CH$_2$)$_2$(N=CMe)$_2$}$_2$(C$_5$H$_3$N)$_2$}Mn$_2$Cl$_3$(MnCl$_4$)]$_n$ present in the crystals of **4**, showing the continuous –Mn–Cl–Mn–Cl–backbone.
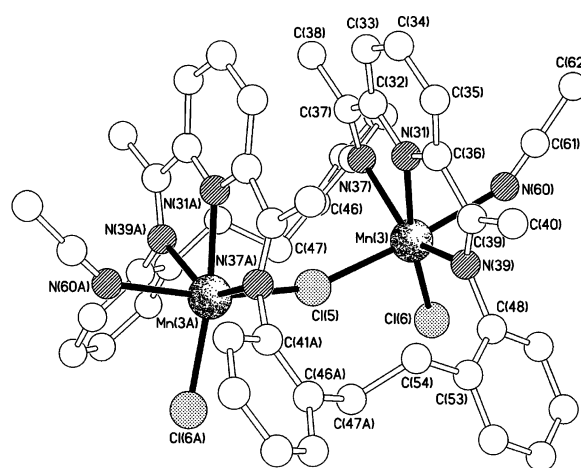
Fig. 7 One of the monomeric [{2,6-{(2′,2″-C$_6$H$_4$–CH$_2$)$_2$(N=CMe)$_2$}$_2$-(C$_5$H$_3$N)$_2$}Mn$_2$Cl$_3$(NCMe)$_2$] cations present in the crystals of **4**.

distorted octahedral with *cis* angles ranging between 72.0(1) and 110.9(1)° in the polymer and 71.0(1) and 108.9(1)° in the monomer (Table 4). In both the polymer and monomer the distances from the manganese to the "axial" chlorine atoms are

Table 4 Selected bond lengths (Å) and angles (°) for **4** ^{a}

Mn(1)–Cl(1)	2.5935(9)	Cl(1)–Mn(1A)	2.5935(9)
Mn(1)–Cl(2)	2.3491(13)	Mn(1)–Cl(3)	2.716(2)
Mn(1)–N(1)	2.168(4)	Mn(1)–N(7)	2.295(4)
Mn(1)–N(9)	2.295(4)	Mn(2)–Cl(3)	2.3806(14)
Mn(2)–Cl(3A)	2.3806(14)	Mn(2)–Cl(4)	2.352(2)
Mn(2)–Cl(4A)	2.352(2)	C(7)–N(7)	1.291(6)
C(9)–N(9)	1.262(6)	Mn(3)–Cl(5)	2.5333(8)
Cl(5)–Mn(3A)	2.5333(8)	Mn(3)–Cl(6)	2.3627(13)
Mn(3)–N(31)	2.201(4)	Mn(3)–N(39)	2.298(4)
Mn(3)–N(37)	2.336(4)	Mn(3)–N(60)	2.388(5)
C(37)–N(37)	1.280(6)	C(39)–N(39)	1.280(6)
N(1)–Mn(1)–N(9)	71.96(14)	N(1)–Mn(1)–N(7)	72.06(14)
N(9)–Mn(1)–N(7)	143.92(14)	N(1)–Mn(1)–Cl(2)	174.58(10)
N(9)–Mn(1)–Cl(2)	110.87(11)	N(7)–Mn(1)–Cl(2)	104.78(10)
N(1)–Mn(1)–Cl(1)	88.76(10)	N(9)–Mn(1)–Cl(1)	85.19(10)
N(7)–Mn(1)–Cl(1)	96.65(10)	Cl(2)–Mn(1)–Cl(1)	96.04(5)
N(1)–Mn(1)–Cl(3)	80.39(11)	N(9)–Mn(1)–Cl(3)	79.93(10)
N(7)–Mn(1)–Cl(3)	91.56(10)	Cl(2)–Mn(1)–Cl(3)	95.43(5)
Cl(1)–Mn(1)–Cl(3)	163.70(5)	Cl(4)–Mn(2)–Cl(4A)	104.89(8)
Cl(4)–Mn(2)–Cl(3A)	114.61(5)	Cl(4A)–Mn(2)–Cl(3A)	111.57(5)
Cl(4)–Mn(2)–Cl(3)	111.57(5)	Cl(4A)–Mn(2)–Cl(3)	114.61(5)
Cl(3A)–Mn(2)–Cl(3)	99.94(8)	Mn(1)–Cl(1)–Mn(1A)	156.71(8)
Mn(1)–Cl(3)–Mn(2)	129.74(6)	N(31)–Mn(3)–N(39)	71.00(14)
N(31)–Mn(3)–N(37)	71.27(14)	N(39)–Mn(3)–N(37)	142.06(14)
N(31)–Mn(3)–Cl(6)	170.79(11)	N(39)–Mn(3)–Cl(6)	108.87(11)
N(37)–Mn(3)–Cl(6)	107.70(10)	N(31)–Mn(3)–N(60)	80.1(2)
N(39)–Mn(3)–N(60)	85.7(2)	N(37)–Mn(3)–N(60)	84.1(2)
Cl(6)–Mn(3)–N(60)	90.74(12)	N(31)–Mn(3)–Cl(5)	90.05(11)
N(39)–Mn(3)–Cl(5)	86.97(10)	N(37)–Mn(3)–Cl(5)	96.92(10)
Cl(6)–Mn(3)–Cl(5)	99.15(5)	N(60)–Mn(3)–Cl(5)	169.20(12)
Mn(3)–Cl(5)–Mn(3A)	159.75(8)		

^{a} Equivalent atoms labelled 'A' are related to their unique counterparts by the crystallographic C_2 axis.
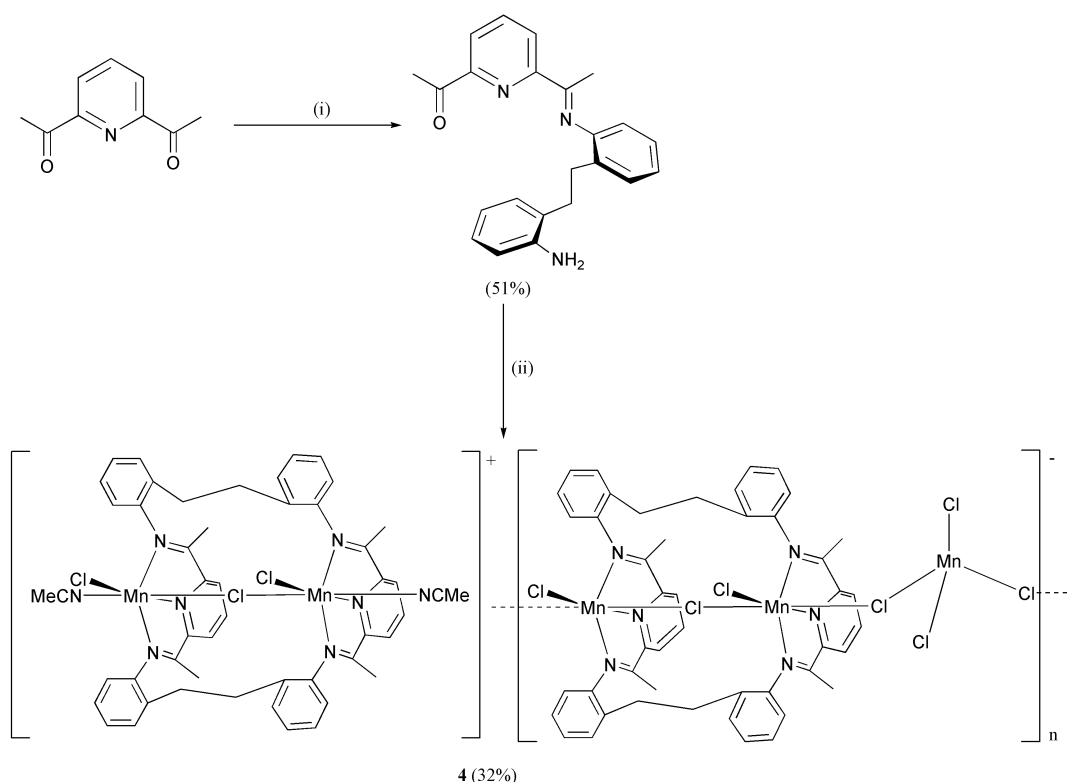
**Scheme 2** Reagents and conditions: (i) $[\{2,2''-(NH_2)C_6H_4\}_2(CH_2CH_2)]$, EtOH, H$^+$, heat; (ii) MnCl$_2$, MeCN, heat.

longer than those to their equatorial counterparts. In the polymer, however, the linkage to the chlorine atom of the MnCl$_4$ dianion is significantly longer [2.716(2) Å] than to that linking the two octahedra [2.594(1) Å]. There is no distinct pattern of differences (monomer *vs.* polymer) in the bonding to the bis(imino)pyridine ligand. In the monomer the bis(imino)-pyridine unit is planar to within 0.07 Å with the manganese atom lying 0.14 Å out of plane and the phenyl rings are both inclined, in the same sense (C_2 rather than C_s symmetric), by *ca.* 63°. In the polymer the bis(imino)pyridine unit is slightly more distorted, being planar to only 0.10 Å but with the manganese atom lying within this plane; the phenyl rings are again inclined in the same sense, here by *ca.* 63 and 71°. The anions and cations pack to form alternating layers within the crystal. A number of transition metal complexes have been prepared that contain the aryl-substituted bis(imino)pyridine

motif (type **A** in Fig. 1) incorporated into a macrocyclic ligand[11] but none have been reported that incorporate the *ortho*-bridged diamine [{2,2′-(NH$_2$)C$_6$H$_4$}$_2$(CH$_2$CH$_2$)]. A tetramanganese complex involving chloride-bridged bimetallic units each sandwiched into a macrocycle has been described[12] as has an infinite polymer based on chloride-bridged [bis(imino)pyridine]Mn units.[13]

Complex **4** shows antiferromagnetic coupling; the magnetic moment, based on the composition of the complex being the cation–anion pair [LMn$_2$Cl$_3$(NCMe)$_2$][LMn$_2$Cl$_3$(MnCl$_4$)], drops from 13.7 μ_B at 300 K to 6.0 μ_B at 6 K as indicated in Fig. 8. The FAB mass spectrum of **4** shows peaks corresponding to
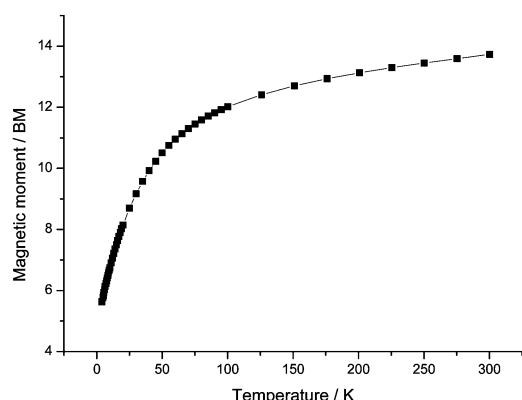
Fig. 8 Plot of magnetic moment against temperature for [{2,6-{(2′,2″-C$_6$H$_4$–CH$_2$)$_2$(N=CMe)$_2$}$_2$(C$_5$H$_3$N)$_2$}Mn$_2$Cl$_3$(NCMe)$_2$][{2,6-{(2′,2″-C$_6$H$_4$–CH$_2$)$_2$(N=CMe)$_2$}$_2$(C$_5$H$_3$N)$_2$}Mn$_2$Cl$_3$(MnCl$_4$)] (**4**).

the fragments LMn$_2$Cl$_3$ and LMn. In the infrared spectrum absorption bands for the C=N stretch are seen *ca.* 1595 cm^{-1}. Microanalytical data support the empirical formula given for **4**.

In conclusion, four manganese complexes based on ligands either containing or derived from the bis(imino)pyridine motif have been prepared and characterised. All the mononuclear complexes (**1–3**) are paramagnetic while the polymetallic complex **4** exhibits antiferromagnetic behaviour. It is worthy of note that, while iron and cobalt analogues of **1–3** can be prepared, iron and cobalt analogues of **4** have not proved accessible.

Experimental

General

All manipulations were carried out under an atmosphere of nitrogen using standard Schlenk and cannula techniques or in a conventional nitrogen-filled glove-box. Solvents were refluxed over an appropriate drying agent, and distilled and degassed prior to use. Elemental analyses were performed by the microanalytical services of the Department of Chemistry at Imperial College and Medac Ltd. NMR spectra were recorded on a Bruker spectrometer at 250 MHz (^{1}H) and 62.9 MHz (^{13}C) at 293 K; chemical shifts are referenced to the residual protio impurity of the deuterated solvent; coupling constants are quoted in Hz. IR spectra (Nujol mulls) were recorded on Perkin-Elmer 577 and 457 grating spectrophotometers. Mass spectra were obtained using either fast atom bombardment (FAB) or electron impact (EI). Magnetic susceptibility studies were performed using an Evans balance (Johnson Matthey) at room temperature. The magnetic moment was calculated following standard methods[14] and corrections for underlying diamagnetism were applied to data.[15]

Materials

The syntheses of [2,6-{(2,4,6-Me$_3$C$_6$H$_2$)N=CMe}$_2$C$_5$H$_3$N], [2,6-{(Me)(Ph)NN=CMe}$_2$C$_5$H$_3$N] and [2-{(2,6-Pr$^i_2$C$_6$H$_3$)N=CH}-6-{(2,6-Pr$^i_2$C$_6$H$_3$)NHCH(Me)}C$_5$H$_3$N] have been reported

elsewhere.[5,7,8,16] Compound [{2,2′-(NH$_2$)C$_6$H$_4$}$_2$(CH$_2$CH$_2$)] was obtained as its diphosphate salt and extracted from aqueous alkaline solution into ethyl acetate, dried (MgSO$_4$) and recrystallised from isopropyl alcohol. All other chemicals were obtained commercially and used as received unless stated otherwise.

Preparations

[2-{(2′-H$_2$NC$_6$H$_4$–C$_2$H$_4$–2″-C$_6$H$_4$)N=CMe}-6-{O=CMe}-C$_5$H$_3$N]. To a solution of 2,6-diacetylpyridine (1.00 g, 6.13 mmol) in absolute ethanol (25 cm^3) was added [{2,2′-(H$_2$N)-C$_6$H$_4$}$_2$(C$_2$H$_4$)] (1.30 g, 6.13 mmol). After addition of a few drops of glacial acetic acid the solution was refluxed for 6 h. Volatiles were removed under reduced pressure and the solid was washed with cold ethanol and dried to give [2-{(2′-H$_2$NC$_6$H$_4$–C$_2$H$_4$–2″-C$_6$H$_4$)N=CMe}-6-{O=CMe}C$_5$H$_3$N] as a yellow solid. Yield: 1.12 g, 51%. EI mass spectrum, *m/z* 357 [M$^+$]. ^{1}H NMR (CDCl$_3$): δ 8.61 [d, ^{3}J(HH) 7.6, Py–H_m, 1H], 8.15 [d, ^{3}J(HH) 7.6, Py–H_m, 1H], 7.95 [app. t, Py–H_p, 1H], 7.3–6.5 [m, Ph, 8H], 3.45 [s, br, NH, 2H], 2.80 [s, MeC=O, 3H], 2.78 [s, CH$_2$CH$_2$, 4H] and 2.41 [s, MeC=N, 3H]. IR (Nujol mull, cm^{-1}): ν(N–H) 3441, ν(C=O) 1696, ν(C=N) 1638. Anal. Calcd. For C$_{23}$H$_{23}$N$_3$O: C, 77.31; H, 6.44; N, 11.76. Found: C, 77.59; H, 6.71; N, 11.45%.

[2,6-{(2,4,6-Me$_3$C$_6$H$_2$)N=CMe}$_2$C$_5$H$_3$N]MnBr$_2$ (1). The ligand [2,6-{(2,4,6-Me$_3$C$_6$H$_2$)N=CMe}$_2$C$_5$H$_3$N] (1.00 g, 2.52 mmol) and MnBr$_2$ (0.54 g, 2.52 mmol) were heated at reflux in acetonitrile (50 cm^3) for 12 h. Following filtration, **1** was obtained as an orange crystalline solid on prolonged standing at ambient temperature. Yield: 1.19 g, 77%. Anal. Calcd. for C$_{27}$H$_{31}$Br$_2$N$_3$Mn: C, 52.96; H, 5.07; N, 6.86. Found: C, 53.10; H, 5.21; N, 6.71%. FAB mass spectrum, *m/z* 612 [M$^+$], 532 [M$^+$ − Br]. IR (cm^{-1}) ν(C=N) 1591. μ_{eff} 5.67 μ_B. EPR (toluene, 298 K): g = 2.00.

[2,6-{(Me)(Ph)NN=CMe}$_2$C$_5$H$_3$N]MnCl$_2$ (2). As for **1**, but using [2,6-{(Me)(Ph)NN=CMe}$_2$C$_5$H$_3$N] (1.00 g, 2.68 mmol) and MnCl$_2$ (0.33 g, 2.62 mmol) gave **2** as orange blocks. Yield: 0.53 g, 40%. Anal. Calcd. for C$_{23}$H$_{25}$Cl$_2$N$_5$Mn: C, 55.53; H, 5.03; N, 14.08. Found: C, 55.71; H, 5.16; N, 13.97%. FAB mass spectrum, *m/z* 498 [M$^+$], 463 [M$^+$ − Cl]. IR (cm^{-1}) ν(C=N) 1592. μ_{eff} 5.69 μ_B. EPR (toluene, 298 K): g = 2.00.

[2-{(2,6-Pr$^i_2$C$_6$H$_3$)N=CH}-6-{(2,6-Pr$^i_2$C$_6$H$_3$)NHCH(Me)}-C$_5$H$_3$N]MnCl$_2$ (3). As for **1**, but using [2-{(2,6-Pr$^i_2$C$_6$H$_3$)-N=CH}-6-{(2,6-Pr$^i_2$C$_6$H$_3$)NHCH(Me)}C$_5$H$_3$N] (1.00 g, 2.13 mmol) and MnCl$_2$ (0.27 g, 2.15 mmol) gave **3** as orange blocks. Yield: 0.95 g, 75%. Anal. Calcd. for C$_{32}$H$_{43}$Cl$_2$N$_3$Mn: C, 64.54; H, 7.23; N, 7.06. Found: C, 64.81; H, 7.56; N, 6.95%. FAB mass spectrum, *m/z* 596 [M$^+$], 561 [M$^+$ − Cl]. IR (cm^{-1}) ν(N–H) 3270, ν(C=N) 1591. μ_{eff} 5.71 μ_B. EPR (toluene, 298 K): g = 2.00.

[{2,6-{(2′,2″-C$_6$H$_4$–CH$_2$)$_2$(N=CMe)$_2$}$_2$(C$_5$H$_3$N)$_2$}Mn$_2$Cl$_3$-(NCMe)$_2$][{2,6-{(2′,2″-C$_6$H$_4$–CH$_2$)$_2$(N=CMe)$_2$}$_2$(C$_5$H$_3$N)$_2$}Mn$_2$-Cl$_3$(MnCl$_4$)]$_n$ (4). As for **1**, but using [2-{(2′-H$_2$NC$_6$H$_4$–C$_2$H$_4$–2″-C$_6$H$_4$)N=CMe}-6-{O=CMe}C$_5$H$_3$N] (1.00 g, 2.80 mmol) and MnCl$_2$ (0.35 g, 2.78 mmol) gave **4** as orange blocks. Yield: 0.37 g, 32% (based on Mn). Anal. Calcd. for C$_{96}$H$_{90}$Cl$_{10}$N$_{14}$Mn$_5$: C, 55.71; H, 4.35; N, 9.48. Found: C, 55.02; H, 3.95; N, 8.51%. FAB mass spectrum, *m/z* 895 [{2,6-{(2′,2″-C$_6$H$_4$–CH$_2$)$_2$-(N=CMe)$_2$}$_2$(C$_5$H$_3$N)$_2$}Mn$_2$Cl$_3$], 732 [{2,6-{(2′,2″-C$_6$H$_4$–CH$_2$)$_2$-(N=CMe)$_2$}$_2$(C$_5$H$_3$N)$_2$}Mn]. IR (cm^{-1}) ν(C=N) 1595.

X-Ray crystal structure determinations

Table 5 provides a summary of the crystallographic data for compounds **1–4**. Data were collected on Siemens P4 diffractometers using ω-scans. The structures were solved by direct methods and they were refined based on F^2 using the

Table 5 Crystal data, data collection and refinement parameters for compounds **1**–**4**[a]

Data	1	2	3	4
Formula	$C_{27}H_{31}N_3Br_2Mn$	$C_{23}H_{25}N_5Cl_2Mn$	$C_{32}H_{43}N_3Cl_2Mn$	$[(C_{46}H_{42}N_6Cl_3Mn_2)(MeCN)_2]$ $[(C_{46}H_{42}N_6Cl_3Mn_2)(MnCl_4)]$
Solvent	MeCN	MeCN	—	6MeCN
Formula weight	653.4	538.4	595.5	2315.3
Colour, habit	Yellow plates	Orange plates	Orange prisms	Orange prisms
Crystal size/mm	$0.50 \times 0.27 \times 0.03$	$0.20 \times 0.20 \times 0.05$	$0.33 \times 0.28 \times 0.22$	$0.63 \times 0.23 \times 0.12$
Temperature/K	293	293	293	173
Crystal system	Monoclinic	Monoclinic	Orthorhombic	Monoclinic
Space group	$P2_1/n$ (no. 14)	$P2_1/c$ (no. 14)	$P2_12_12_1$ (no. 19)	$P2/c$ (no. 13)
a/Å	16.842(1)	13.737(1)	13.463(1)	12.796(1)
b/Å	15.156(1)	13.211(1)	13.559(1)	17.298(1)
c/Å	23.431(2)	15.181(1)	18.694(1)	25.167(1)
β/°	92.04(1)	101.91(1)	—	94.43(1)
V/Å³	5977.1(5)	2695.5(3)	3412.3(4)	5553.6(7)
Z	8[b]	4	4	2[c]
Radiation used	Cu-Kα	Cu-Kα[d]	Cu-Kα	Cu-Kα[d]
μ/mm^{-1}	6.90	5.99	4.75	7.15
No. of unique reflections				
measured	8194	3982	3176	8230
observed, $|F_o| > 4\sigma(|F_o|)$	5248	2650	2691	5746
Absorption correction	Lamina	Ellipsoidal	Ellipsoidal	Empirical
No. of variables	677	284	348	674
R_1, wR_2[e]	0.059, 0.133	0.059, 0.121	0.041, 0.090	0.052, 0.108

[a] Details in common: graphite monochromated radiation, refinement based on F^2. [b] There are two crystallographically independent molecules in the asymmetric unit. [c] The complex has crystallographically C_2 symmetry. [d] Rotating anode source. [e] $R_1 = \Sigma||F_o| - |F_c||/\Sigma|F_o|$; $wR_2 = \{\Sigma[w(F_o^2 - F_c^2)^2]/\Sigma[w(F_o^2)^2]\}^{1/2}$; $w^{-1} = \sigma^2(F_o^2) + (aP)^2 + bP$.

SHELXTL program system.[17] The structure of **3** was shown to be a partial racemic twin by a combination of *R*-factor tests [$R_1^+ = 0.0549$, $R_1^- = 0.0603$] and by use of the Flack parameter [$x^+ = +0.45(5)$, $x^- = +0.55(5)$]—the refinements using the Flack parameter gave the substantially lower residuals quoted in the table.

CCDC reference numbers 190871–190874.

See http://www.rsc.org/suppdata/dt/b2/b207384f/ for crystallographic data in CIF or other electronic format.

Acknowledgements

References

1 (*a*) M. Bochmann, *J. Chem. Soc., Dalton Trans.*, 1996, 255; (*b*) W. Kaminsky, *J. Chem. Soc., Dalton Trans.*, 1998, 255; (*c*) H.H. Brintzinger, D. Fischer, R. Mülhaupt, B. Rieger and R. M. Waymouth, *Angew. Chem., Int. Ed. Engl.*, 1995, **34**, 1143; (*d*) A. A. Montagna, R. M. Burkhart and A. H. Dekmezian, *CHEMTECH*, 1997, December 26.

2 S. D. Ittel, L.K. Johnson and M. Brookhart, *Chem. Rev.*, 2000, **100**, 1169.

3 G. J. P. Britovsek, V. C. Gibson and D. F. Wass, *Angew. Chem., Int. Ed.*, 1999, **38**, 429.

4 S. Mecking, *Angew. Chem., Int. Ed.*, 2001, **40**, 534.

5 (*a*) G. J. P. Britovsek, V. C. Gibson, B. S. Kimberley, P. J. Maddox, S. J. McTavish, G. A. Solan, A. J. P. White and D. J. Williams, *Chem. Commun.*, 1998, 849; (*b*) G. J. P. Britovsek, M. Bruce, V. C. Gibson, B. S. Kimberley, P. J. Maddox, S. Mastroianni, S. J. McTavish, C. Redshaw, G. A. Solan, S. Strömberg, A. J. P. White and D. J. Williams, *J. Am. Chem. Soc.*, 1999, **121**, 8728; (*c*) G. J. P. Britovsek, B. A. Dorer, V. C. Gibson, B. S. Kimberley and

G. A. Solan, BP Chemicals Ltd, *WO patent 99/12981*, 1999; (*Chem. Abstr.*, 1999, **130**, 252–793).

6 (*a*) B. L. Small, M. Brookhart and A. M. A. Bennett, *J. Am. Chem. Soc.*, 1998, **120**, 4049; (*b*) B. L. Small and M. Brookhart, *J. Am. Chem. Soc.*, 1998, **120**, 7143.

7 G. J. P. Britovsek, V. C. Gibson, B. S. Kimberley, S. Mastroianni, C. Redshaw, G. A. Solan, A. J. P. White and D. J. Williams, *J. Chem. Soc., Dalton Trans.*, 2001, 1639.

8 (*a*) G. J. P. Britovsek, V. C. Gibson, S. Mastroianni, D. C. H. Oakes, C. Redshaw, G. A. Solan, A. J. P. White and D. J. Williams, *Eur. J. Inorg. Chem.*, 2001, 431; (*b*) V. C. Gibson, B. S. Kimberley and G. A. Solan, BP Chemicals Ltd., *WO patent 00/20427*, 2000; (*Chem. Abstr.*, 2000, **132**, 279–649f).

9 D. Reardon, G. Aharonian, S. Gambarotta and G. P. A. Yap, *Organometallics*, 2002, **21**, 786.

10 D. A. Edwards, M. F. Mahon, W. R. Martin, K. C. Molloy, P. E. Fanwick and R. A. Walton, *J. Chem. Soc., Dalton Trans.*, 1990, 3161.

11 See, for example, (*a*) N. W. Alcock, D. C. Liles, M. McPartlin and P. A. Tasker, *J. Chem. Soc., Chem. Commun.*, 1974, 727; (*b*) L. Valencia, H. Adams, R. Bastida, A. de Blas, D. E. Fenton, A. Macias, A. Rodriguez and T. Rodriguez-Blas, *Inorg. Chim. Acta*, 2000, **300**, 234; (*c*) D. C. Liles, M. McPartlin and P. A. Tasker, *J. Chem. Soc., Dalton Trans.*, 1987, 1631; (*d*) D. E. Fenton, R. W. Matthews, M. McPartlin, B. P. Murphy, I. J. Scowen and P. A. Tasker, *J. Chem. Soc., Chem. Commun.*, 1994, 1391; (*e*) R. W. Matthews, M. McPartlin and I. J. Scowen, *J. Chem. Soc., Dalton Trans.*, 1997, 2861.

12 S. Brooker and V. McKee, *J. Chem. Soc., Chem. Commun.*, 1989, 619.

13 B. C. Unni Nair, J. E. Sheats, R. Ponteciello, D. Van Engen, V. Petrouleas and G. C. Dismukes, *Inorg. Chem.*, 1989, **28**, 1582.

14 M. B. Mabbs and D. J. Machin, *Magnetism and Transition Metal Complexes*, Chapman and Hall, London, 1973.

15 C. J. O'Connor, *Prog. Inorg. Chem.*, 1982, **29**, 203; *Handbook of Chemistry and Physics*, ed. R. C. Weast, CRC Press, Boca Raton, FL, 70th edn., 1990, p. E134.

16 M. Bruce, V. C. Gibson, C. Redshaw, G. A. Solan, A. J .P. White and D. J. Williams, *Chem. Commun.*, 1998, 2523.

17 SHELXTL PC version 5.03, Siemens Analytical X-Ray Instruments, Inc., Madison, WI, 1994; SHELXTL PC version 5.1, Bruker AXS, Madison, WI, 1997.